2019

EFFECTS OF INCORPORATING INERTIAL MEASUREMENTS ON THE LOCALIZATION ACCURACY OF THE SEAGLIDER AUV

Wendy Snyder
University of Rhode Island, wesnyder11@gmail.com

EFFECTS OF INCORPORATING INERTIAL MEASUREMENTS ON THE LOCALIZATION ACCURACY OF THE SEAGLIDER AUV

BY

WENDY SNYDER

A THESIS SUBMITTED IN PARTIAL FULFILLMENT OF THE

REQUIREMENTS FOR THE DEGREE OF

MASTER OF SCIENCE

IN

OCEAN ENGINEERING

UNIVERSITY OF RHODE ISLAND

2019

MASTER OF SCIENCE THESIS

OF

WENDY SNYDER

APPROVED:

Thesis Committee:

Major Professor Lora Van Uffelen

Stephen Licht

Paolo Stegagno

Martin Renken

Nasser H. Zawia

DEAN OF THE GRADUATE SCHOOL

UNIVERSITY OF RHODE ISLAND

2019

ABSTRACT

The Kongsberg Seaglider M1 is a commercially available autonomous underwater vehicle (AUV) primarily used as a platform for oceanographic measurements of salinity, temperature, and oxygen. The Seaglider currently uses two different dead-reckoned solutions, the glide slope model (GSM) and the hydrodynamic model (HDM), to provide a localization solution for each dive. While the accuracy of these solutions was not previously known explicitly, for the purposes of oceanographic profiling they were generally deemed sufficient. As the platform matures, there has been a growing interest in expanding its application and measurement capabilities. With some of the desired new applications, such as using the Seaglider as a moving acoustic receiver in acoustic tomography, comes a need to quantify and improve the localization accuracy of the vehicle.

This project sought to quantify the accuracy of the two localization solutions currently in use, investigate the effects of additional inertial measurements on the accuracy of such solutions, and identify potential opportunities for improvement to vehicle localization. To accomplish these goals, a Seaglider was instrumented with an inertial measurement unit (IMU) and tracked on the Dabob Bay acoustic tracking range. The acoustic track from the range was considered a ground-truth and used to evaluate various localization solutions. Error metrics were developed to quantify and compare the accuracy of the different localization solutions.

Results indicated the Seaglider's GSM solution is significantly more accurate than the HDM solution; while additional inertial measurements did not improve the accuracy of these solutions. From the collected data, sources of error in the two main localization solutions were identified, as well as their expected magnitude. Results were then used to make recommendations for development of an improved localization solution.

ACKNOWLEDGMENTS

This research would not have been possible without the effort and support of many people. I would first like to thank Dr. Lora Van Uffelen, my major professor, for her time, guidance, and support during my time at University of Rhode Island. I would also like to thank Martin Renken, my NUWC mentor, for his time and effort in making the fieldwork required for this research possible. Furthermore I would like to thank the other members of my thesis committee, Dr. Stephen Licht, Dr. Paolo Stegagano, and Dr. Mingxi Zhou.

Special thanks to Rich Patterson, Liz Creed, John Faust, and the rest of the Seaglider team at Kongsberg Underwater Technologies Inc. for their support and assistance with sensor integration and data logging on the Seaglider, as well as the Range Officers from NUWC Keyport for their assistance with data collection. Thanks also to Sarah Webster at APL-UW for being willing to answer my many questions. The support of KVH industries and Lord Microstrain was also greatly appreciated in bringing this work to fruition.

I am grateful to the Science Mathematics and Research for Transformation (SMART) scholarship program for their financial support of my education. The SMART program also enabled opportunities to develop collaborations with NUWC Keyport and focus my research in a way that conformed to overlapping interests of the parties involved.

Finally I would like to thank my family and friends. I would not be where I am today without their endless support. Extra thanks to Will, who first encouraged me to explore the world of ocean engineering and was always happy to provide his expertise and input throughout the research process.

PREFACE

This thesis was prepared in the manuscript format and includes two manuscripts and one appendix. Formatting of both manuscripts has been modified to meet university requirements, but all content is identical to that in submitted manuscripts. The author of this thesis was the lead investigator and lead author of both included manuscripts.

The first manuscript has been submitted for publication in IEEE Oceans conference proceedings © 2019 IEEE. Reprinted, with permission, from W. Snyder, L. Van Uffelen, and M. Renken, "Effects of incorporating inertial measurements on the localization accuracy of the Seaglider AUV," *Oceans 2019*, 2019. It provides an overview of current Seaglider localization methods as well as the development of an acoustic tracking experiment to evaluate localization solutions. Preliminary results from the experiment are presented focusing on quantifying accuracy in the current Seaglider localization models and the effects of incorporating an inertial attitude and heading reference system on those solutions.

The second manuscript expands on the work presented in the first manuscript and is formatted with the intent of future publication in the IEEE Journal of Oceanic Engineering © 2019 IEEE. It includes results from a number of additional inertial attitude estimators as well as an in-depth analysis of potential sources of error in the localization solutions.

The appendix includes a section with results not presented in the manuscripts from an additional simulation using a fiber-optic gyroscope.

TABLE OF CONTENTS

Page

LIST OF FIGURES

LIST OF TABLES

CHAPTER 1

"Effects of Incorporating Inertial Measurements on the Localization Accuracy of the Seaglider AUV"

by Wendy Snyder[1], Lora Van Uffelen[2], and Martin Renken[3]

is submitted to the IEEE Oceans conference proceedings 2019[4].

[1]Masters Candidate, Department of Ocean Engineering, The University of Rhode Island, Narragansett, RI 02882, Email: wendy_snyder@my.uri.edu

[2]Assistant Professor, Department of Ocean Engineering, The University of Rhode Island, Narragansett, RI 02882

[3]Naval Undersea Warfare Center Division Keyport, Keyport, WA, 98345

[4]DISTRIBUTION A. Approved for public release: distribution unlimited. NUWC Keyport #19-005

Abstract

Seaglider is a buoyancy driven autonomous underwater vehicle (AUV) primarily used as a platform for oceanographic measurements of salinity, temperature, and oxygen, where precise localization is not crucial. A recent experiment tracked a Seaglider, instrumented with an attitude and heading reference system (AHRS), on an acoustic tracking range in an effort to quantify the accuracy of the Seaglider's two localization solutions and determine the effects of incorporating additional inertial measurements into the solution.

Preliminary analysis of results has shown the Seaglider's glide slope model (GSM) is more accurate and reliable than the hydrodynamic model (HDM) during typical flight dynamics. Errors in the GSM solution did not exhibit a clear drift behavior but remained on average within 22 m of the ground truth acoustic track over dives with a maximum depth of 90 to 125 m. Errors in the HDM solution exhibited linear growth until the apogee point of the dive when errors began to linearly reduce. On average the error increased at a rate of about 5 m/min between the surface and maximum dive depth, with maximum errors in excess of 100 m during dives with a maximum depth of 90 m. The substitution of attitude estimates from the AHRS into the localization models provided similar but less consistent results with slightly higher errors.

1.1 Introduction

The Seaglider AUV falls into the class of AUVs known as gliders. Gliders are buoyancy driven AUVs which typically operate in the mid-water following a sawtooth dive tracjectory. Gliders are capable of collecting a wide variety of oceanographic data such as temperature, salinity, and oxygen profiles for months at a time with relatively little mission support, making them a powerful platform for oceanographic research [1]. Recently there has been a growing interest in

using gliders as moving acoustic receivers in acoustic tomography experiments [2]. Such experiments rely on time-of-flight measurements of acoustic signals in which accurate glider localization becomes critical to resolve the fundamental ambiguity between position and sound velocity. Currently, underwater position errors in glider localization based on glider hydrodynamic models alone are estimated to be on the order of 600 – 900 m rms for dives to 1000 m [3].

Glider position errors can be reduced to less than 100 m rms using transmissions from acoustic tomography sources at ranges up to several hundred kilometers [3]; however the sources typically only transmit once every few hours while gliders are underwater for several hours at a time. This method also requires the presence of a long-range acoustic transceiver array which limits the navigable region and significantly increases the complexity and cost of deployment. Even in cases where an acoustic transceiver array is feasible, it is still desirable to improve position estimates between acoustic position fixes to better capture the full dive trajectory of the glider. In addition to applications of gliders as acoustic receivers, improvements in glider localization would also improve the ability to navigate under ice and would provide better spatial precision for collected oceanographic data.

Many unmanned underwater vehicles (UUVs) utilize an inertial navigation system (INS) aided by a doppler velocity log (DVL) to navigate underwater between position updates from GPS or acoustic navigation systems. For vehicles operating within 200 – 300 m of the seafloor, inertial navigation systems with DVL aiding have been refined such that $\sim$0.2% distance traveled position error growth (2σ) is possible [4]. In the mid-water, inertial navigation becomes more difficult since DVLs cannot achieve bottom lock to track the vehicle's speed over ground causing the INS to drift rapidly. As a result, many AUVs and ROVs rely on acoustic tracking methods when operating in the midwater or during long descents

to the seafloor. These methods are limiting in that they provide position updates with relatively low frequency, can be noisy, and require either continued presence of a dedicated surface vessel or a time-consuming transponder deployment [4].

Gliders were primarily developed as a platform to collect oceanographic measurements such as temperature and salinity at a fraction of the cost of oceanographic research vessels. For such oceanographic observations, the simple dead-reckoned and hydrodynamic models used for glider localization between GPS fixes at the surface typically offer sufficient accuracy position estimates. Gliders are also designed to be relatively small and low power to enable them to complete long endurance missions, traveling approximately 0.5 knots while using only about 0.5 W of power. An INS similar to those typically used by other UUVs would be much too large and require too much power for use on a glider. It is only more recently with the desire to use gliders for applications requiring more precise localization and the development of small, low power IMUs that inertial navigation has become a realistic avenue for glider technology.

1.2 Seaglider Flight Models

Processed dive data from the Seaglider provides two different estimates of the vehicle dive trajectory based on two different dive models. The solutions from these two models are often significantly different over the course of a single dive. During this experiment, discrepancies between the models in excess of 100 m were observed over relatively short 30 minute dives to maximum depths of 100 m. Previous analysis during a long range acoustic propagation experiment found the Seaglider's glide slope model to be slightly more consistent with acoustic position fixes than the hydrodynamic model [3].

Both of the Seaglider's models are based on a hydrodynamic flight model for the vehicle which considers steady flight dynamics with slowly varying control

states. The hydrodynamic relations are given as

$$(ql^2)^2 bq^{-(1/4)} - Bql^2 \sin(\theta) + B^2 ca^{-2} \cos^2(\theta) = 0 \tag{1.1}$$

$$c\alpha^2 + a\alpha \tan(\theta) + bq^{-(1/4)} = 0 \tag{1.2}$$

where q is the dynamic pressure, l is the vehicle length, B is the buoyant force, θ is the glide angle, α is the angle of attack, and a, b, and c are experimentally determined hydrodynamic coefficients [1]. Equations for buoyancy, dynamic pressure, and angle of attack can be derived from these equations by approximating them as quadratic in B, q, and α.

Both models rely on the above hydrodynamic flight model, however the GSM assumes a constant water density throughout each dive and cancels out the buoyancy while the hydrodynamic model uses additional information from the vehicle sensors in order to incorporate time-varying estimates of buoyancy into the model and estimate time-varying dynamic pressure.

1.2.1 Glide Slope Model

The glide slope model uses data from the vehicle's compass, GPS, and pressure sensor to estimate the dive trajectory. The pressure measurements are used to determine depth. The depth rate of change then serves as an estimate of the vertical velocity of the vehicle throughout the dive. Dynamic pressure is expressed as a function of the glide angle and vertical velocity

$$q = \frac{\rho_0}{2} \left(\frac{w}{\sin(\theta)} \right)^2, \tag{1.3}$$

where ρ_0 is a constant reference water density and w is the vertical velocity of the Seaglider [1]. Combining (1.2) with (1.3) results in a simplified model where the glide angle and angle of attack are the only unknowns.

The vehicle pitch given by the vehicle compass is taken as the first guess of the glide slope and used to iteratively solve for the glide slope based on (1.2) and

the relation

$$\theta = \Theta - \alpha, \tag{1.4}$$

where Θ is the measured pitch of the glider. Once the glide slope estimate converges, or a max number of iterations are completed, the total speed and horizontal component of the speed are estimated based on the glide slope and vertical velocity. Using trigonometric relations and dead reckoning techniques, the estimated horizontal speed is then combined with the heading measurement to determine the North and East displacements at each time step.

The cumulative sum of displacements in both the North and East directions for the full dive is then compared to the North and East displacements based on GPS fixes at the start and end of the dive. The difference in the displacements is used to estimate the depth averaged current (DAC) and subsequently correct the displacement estimates at each time step before they are converted to latitude and longitude positions.

1.2.2 Hydrodynamic Model

The main difference between the glide slope model and the hydrodynamic model is the incorporation of variable buoyancy and dynamic pressure estimates. The model uses temperature and salinity data from the vehicle's conductivity temperature (CT) sail to estimate in-situ water density, and information from the variable buoyancy device (VBD) control system to estimate the volume of the vehicle. Buoyancy is then estimated using the computed water density, volume, and other measured constants such as the vehicle mass.

Quadratic approximations of (1.1) and (1.2) are then used to solve iteratively for both the dynamic pressure and glide slope using the buoyancy, vertical velocity and pitch angle. Once the iteration converges or reaches a maximum number of iterations, the total speed is estimated using the computed dynamic pressure.

The glide slope and total speed are then used to estimate velocity components, displacements, DAC, and ultimately latitude and longitude locations as in the glide slope model.

1.3 Methods

1.3.1 Sensor Selection

The Seaglider currently uses a Sparton SP3004D compass to estimate the attitude and heading angles used in the localization models. The Sparton SP3004D consists solely of accelerometers and magnetometers, and thus relies on leveling equations and magnetic heading estimates to determine attitude [5].

Selection of the IMU for integration and testing on the Seaglider aimed to provide a more accurate estimate of vehicle attitude and motion than the current compass without introducing excessive power or space requirements. Sensor options were first selected to ensure they met the size and power constraints of the glider platform and would be capable of measuring in the desired range without significant signal to noise issues. Once a number of sensor options had been identified, specifications were compared to determine the final sensor selection. For AHRS sensors, the attitude accuracy was directly compared to that of the current glider compass to determine expected improvements. Additionally, the noise and bias instability characteristics of the individual accelerometers and gyroscopes in each sensor were compared as these error sources are large contributors to INS drift in the horizontal directions [6]. The sensor selection ultimately weighed all these factors to find the sensor with the best expected performance improvements without excessive power consumption or added cost.

The Lord Sensing 3DM-GX5-25 attitude and heading reference system (AHRS) was selected for integration on the Seaglider. The Lord AHRS is a micro-electro-mechanical system (MEMS) which incorporates three axes mea-

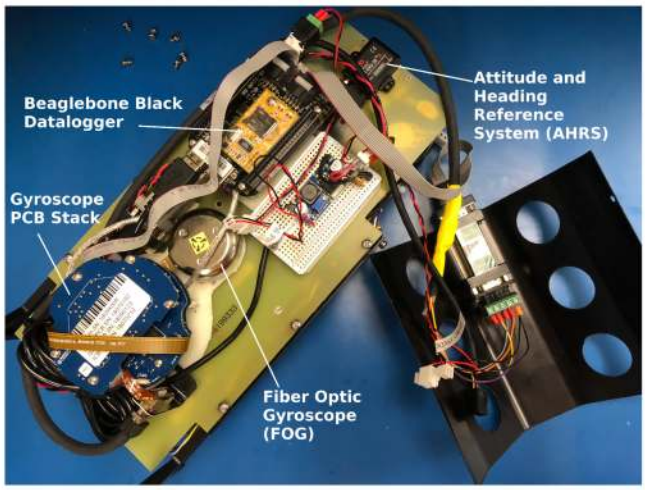

Figure 1.1: Sensor and datalogging package as installed on the Seaglider for the Dabob Bay ground truth tracking experiment.

surements from magnetometers, accelerometers, and gyroscopes into an Extended Kalman Filter (EKF) to estimate attitude and heading. Raw measurement outputs and a variety of other computed outputs are also available from the sensor as desired. The Lord sensor provides many improvements over the current compass including a significant reduction in accelerometer noise density, a 20% improvement in heading accuracy, and a higher attitude output resolution.

The Lord AHRS was powered via the 15 V power supply on the Seaglider and has an estimated power draw of 500 mW. Data were provided via a serial interface connected to an independent datalogger for proof of concept testing. During testing, the sensor and datalogger were mounted in the secondary battery cage along with a single axis fiber optic gyroscope which unfortunately did not properly log any data during the experiment. The layout of the sensors and datalogger as they were mounted in the Seaglider battery housing is shown in Figure 1.1.

1.3.2 Field Deployment

The Seaglider, instrumented with the additional sensors, was deployed in Dabob Bay, WA to collect data necessary for determining the effectiveness of the

alternative sensors in localizing the glider. In order to determine the accuracy and precision of the various localization solutions, a ground truth measurement of the actual vehicle location throughout operation is needed to serve as a reference. For this experiment, the short baseline acoustic tracking system on the Dabob Bay acoustic tracking range operated by the Naval Undersea Warfare Center Division Keyport was used to generate a ground truth. Once drift corrections are applied, the acoustic tracking uncertainty is much smaller than that expected for the inertial solutions and the acoustic track can be used as a reliable ground truth measurement.

Data collection was carried out over three days in September of 2018 on the Dabob Bay acoustic tracking range. During testing, the Seaglider maneuvered between a planned set of way-points around the range. The glider collected its standard dive log files which include compass data from the standard glider compass and GPS fixes at the start and end of each dive. Additionally, inertial data from the Lord AHRS were logged using the independent datalogger. The vehicle continued diving on the range overnight, however acoustic tracking was recorded only during daytime range operations.

The glider was deployed for approximately 68 hours, during which time it completed 86 dives. Of these dives, only 19 had acoustic tracking data for the full dive. Target dive depths varied between 45 m and 126 m depending on the water depth in the area as well as mission requirements. Two sets of in-water compass calibration dives were performed during overnight operation to provide necessary data for calibration of the Sparton compass.

1.3.3 Data Analysis

From the data collected during the field deployment, the accuracy and precision of the current glider models were evaluated and compared to the model

estimates using attitude inputs from the Lord AHRS. For each tracked dive, the latitude and longitude from the ground truth track and the Seaglider models were projected onto a Cartesian coordinate system with an origin located at the GPS location recorded by the Seaglider at the start of the dive.

Localization solutions were then interpolated to the time steps from the range track and the distance between each ground truth track location and the corresponding location estimate was computed. A variety of metrics were developed to quantify the errors in the various solutions and compare the accuracy and precision of each solution. The maximum error (in m) for each tracked dive was selected as the first error metric. To account for difference in dive duration, the maximum error for each dive was also normalized by the distance traveled during the dive. The resulting metric represents the maximum error as a percent of the total distance traveled. The distance traveled during the dive was determined by integrating along the range track of the Seaglider throughout the dive. Finally, the root mean square (rms) error between the range track and localization solution was also computed for each dive as a third error metric. For each localization solution, the average and standard deviation for each of these error metrics were computed across all tracked dives. Three of the tracked dives were excluded when computing average metrics as they were flagged for having atypical flight dynamics due to issues with the VBD system.

1.4 Results

Before comparing results of the GSM and HDM localization solutions, the attitude estimates of the Lord AHRS were first compared to those generated by the Seaglider Sparton compass. The Lord attitude estimates were taken from the device's built-in Extended Kalman Filter (EKF). The EKF had an update rate of 500 Hz, but was only recorded at 10 Hz which was deemed sufficient considering

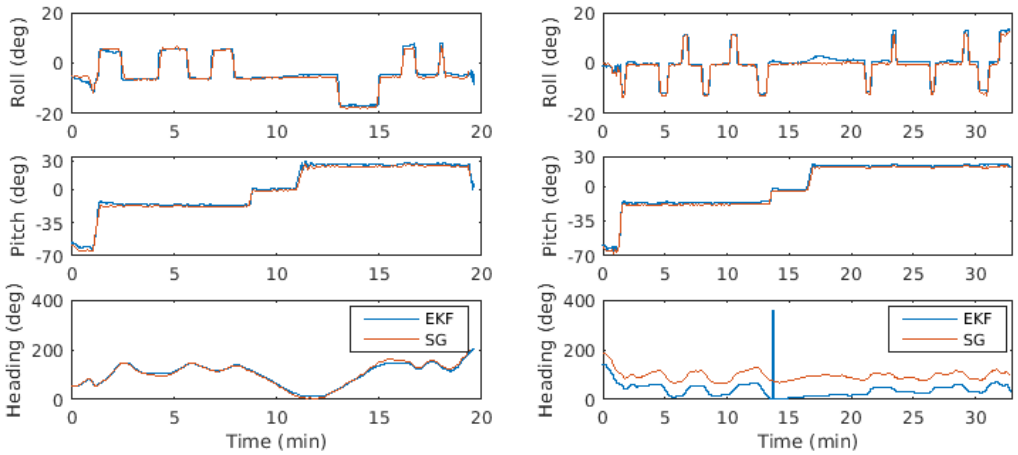

(a) Dive 2 (b) Dive 69

Figure 1.2: Comparison of output from the built-in EKF on the Lord AHRS and the attitude estimates based on the Sparton compass for two dives.

the Seaglider's slow maneuvers. At the manufacturer's recommendation, auto-initialization and auto-calibration settings were used on the EKF.

There was an average pitch offset between the sensors of 1.6 deg, indicating there may have been a slight alignment error when the Lord sensor was mounted. There was also an average roll offset of about 1 deg during the upcast portion of the dive and 0.2 deg during the downcast portion of the dive. Larger discrepancies in pitch and roll angle occurred occasionally, most often at the apogee point of the dive. The heading measurements output by the EKF were at times extremely close to those measured by the Seaglider compass and at other times exhibited a significant offset. Attitude estimates from two dives, one where the EKF closely matched the Seaglider compass (Dive 2) and one in which a heading bias occurred (Dive 69), are shown in Figure 1.2. A discrepancy in the roll angle near apogee (approximately the 18 min. mark) is also present in the data from Dive 69.

These attitude estimates were used as inputs in the Seaglider's GSM and HDM to develop localization solutions for comparison to the range track. A 3-D plot of the Seaglider's path through the water from the acoustic tracking system

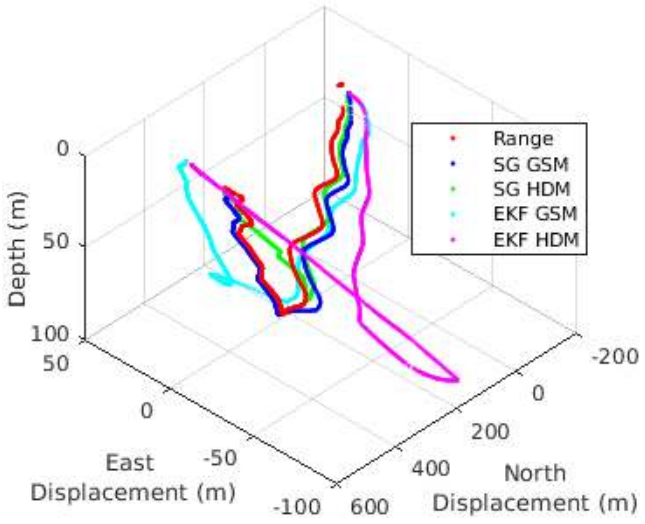

Figure 1.3: 3D plot of the dive trajectory for dive 69 as measured by the acoustic ground truth track and computed localization solutions

and various localization solutions for Dive 69 is shown in Figure 1.3. While the shape of the GSM paths closely follow that of the range track, paths from the HDM solution drift rapidly away from the ground truth until the deepest point of the dive, where they start to converge back toward the range track.

Figure 1.4 shows the localization error versus time from Dive 2 and Dive 69 for both the Seaglider's solutions and the EKF-based models. Dive 2 is an example of a dive where the heading measurements from the two compasses were in agreement, while Dive 69 is an example of when a significant bias was present between the two heading estimates (as shown previously in Figure 1.2).

From the error plots, it is evident that error in the GSM solution is smaller and more constrained than in the HDM where errors grow rapidly with depth and distance from surface GPS fix. Additionally, performance of the EKF-based solutions for Dive 2 was close to, and at times exceeded, that of the solutions using the Seaglider compass. In Dive 69, the errors in the EKF based models are larger than the corresponding Seaglider model throughout the entirety of the dive. This indicates the heading bias present in the EKF solution was likely an error in the

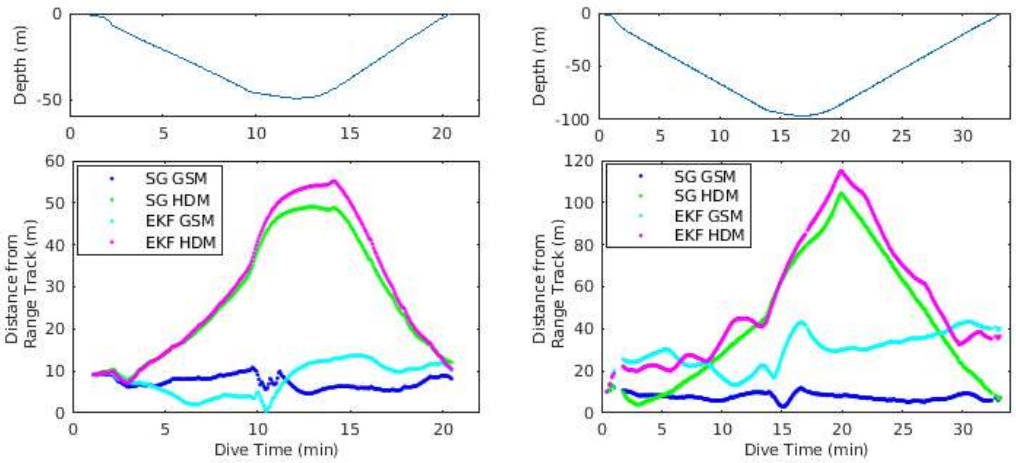

(a) Dive 2 (b) Dive 69

Figure 1.4: Depth vs time (upper) and distance of calculated solutions from the acoustic ground truth range track (lower) for two dives.

Table 1.1
Average Error Metrics (with 1σ standard deviation)

	SG GSM	SG HDM	EKF GSM	EKF HDM
Max Error (m)	21.6 (5.6)	103.8 (33.4)	52.6 (26.4)	112.6 (32.9)
RMS Error (m)	12.7 (3.5)	57.9 (17.4)	32.9 (16.4)	66.7 (21.1)
% Total Distance	4.3 (1.9)	19.1 (3.6)	9.4 (3.8)	21.0 (3.9)

solution of the EKF and not an error in the Seaglider compass.

The error metrics computed for each solution are shown in Table 1.1. In comparing these metrics, the EKF-based models had higher errors and performed less consistently than the current Seaglider models. The GSM solution also outperformed the HDM model in both cases.

1.5 Discussion

The accuracy of the Seaglider's localization solutions was quantified from data collected during the experiment on Dabob Bay. The GSM solution was more accurate than the HDM in all cases. In comparing intermediate outputs from the two models, the HDM and GSM solutions had very similar estimates of glide

slope but a noticeable discrepancy in the velocity estimates throughout much of the dive. The vertical velocity output by the HDM solution also differed from the depth rate of change based on the pressure sensor. While the vertical velocity is not used directly in the dead-reckoned solution, the discrepancy in vertical velocity is indicative of an error with the overall HDM velocity estimate from which the horizontal and vertical velocities are derived. The underestimate of velocity during the downcast portion of the dive, and overestimate during the upcast portion likely contribute a significant portion of the error in the HDM solutions.

In all solutions, errors in the GPS fixes at the start and end of the dive introduced errors. There is also a one to two minute gap between the GPS fix and the start or end of the computed localization solution during which time the Seaglider is drifting on the surface. This gap introduces additional error at the start and end of the dive as the solutions assume the glider is in a fixed location when in reality it is most likely moving in the surface currents. These errors are observable from the errors present in the glider solutions at the start and end of the dive.

Errors in the GSM solutions also tended to exhibit a spike near the apogee point of the dive which corresponded to a spike in the horizontal velocity estimate. The GSM largely relies on the assumption that the glide slope and heading provide the direction of the Seaglider's motion. This assumption allows the vertical velocity from the depth rate of change to be used in estimating horizontal velocity. However near apogee, the glider approaches a nearly horizontal pitch at which point a discontinuity occurs in the velocity relation. Under these conditions, the assumptions of the model likely do not hold and as a result, horizontal velocity estimates from the model become artificially high introducing error into the solution. At shallow pitch angles, because of the model's rapid change in velocity with

pitch angle, velocity estimates are also more sensitive to errors in the pitch angle making attitude accuracy more important at the apogee phase of the dive.

Should opportunities for further field testing arise, it would be ideal to reconfigure the system datalogger to log continuously throughout the dive. The Seaglider's logger interface created a short gap in the logged inertial data at apogee when the log file switches between downcast and upcast. Capturing data during this critical portion of the dive profile would be useful in gaining further insight into the flight dynamics during apogee and ultimately improving the localization solutions.

Based on the results of this experiment, the introduction of an AHRS to the Seaglider did not improve the accuracy of the Seaglider localization estimates. In comparing attitude estimates from the two compasses, it is believed that the Lord EKF was not adequately tuned for the purposes of this experiment, especially the auto-magnetic calibration parameters. Additionally, the consistent pitch offset between the two sensors indicate there may have been some misalignment between the sensor and vehicle. In general however, this may also be an indication that attitude errors are not a significant source of error in vehicle localization relative to other error sources. Of all attitude estimates, the heading most likely has the most significant effect on the accuracy of localization as was observed in comparing solutions from Dive 2 and Dive 69.

Future analysis of the Dabob Bay dataset will utilize raw inertial measurements from the Lord AHRS to develop alternative attitude estimates for input into the Seaglider hydrodynamic models. Such estimators can be better tuned than the built-in EKF and will take advantage of the limited dynamic accelerations present in Seaglider flight.

Acknowledgment

The authors would like to thank the Seaglider group at Kongsberg Underwater Technologies Inc for their assistance with the integration of the sensor and datalogger on the Seaglider, the Naval Undersea Warfare Center Division Keyport for their support of the acoustic range tracking experiment and the University of Rhode Island Ocean Engineering Department.

This project was completed as part of Wendy Snyder's Master's thesis under the support of the Science, Mathematics, and Research for Transformation (SMART) scholarship program.

List of References

[1] C.C. Eriksen, T.J. Osse, R.D. Light, T. Wen, T.W. Lehman,P.L. Sabin, J.W. Ballard, A.M. Chiodi, "Seaglider: A long-range autonomous underwater vehicle for oceanographic research," *IEEE Journal of Oceanic Engineering*, 2001.

[2] L. J. Van Uffelen, E. M. Nosal, B. M. Howe, G. S. Carter, P. F. Worcester, M. A. Dzieciuch, K. D. Heaney, R. L. Campbell, P. S. Cross, "Estimating uncertainty in subsurface glider position using transmissions from fixed acoustic tomography sources," *Journal of the Acoustical Society of America*, 2013.

[3] L. J. Van Uffelen, B. M. Howe, E. M. Nosal, G. S. Carter, P. F. Worcester, M. A. Dzieciuch, "Localization and subsurface position error estimation of gliders using broadband acoustic signals at long range," *IEEE Journal of Oceanic Engineering*, 2016.

[4] L. Medagoda, S. B. Williams, O. Pizarro, J. C. Kinsey, and M. V. Jakuba, "Mid-water current aided localization for autonomous underwater vehicles," *Autonomous Robots*, 2016.

[5] *Sparton Digital Compass User Interface Document*, Sparton Electronics, August 2009.

[6] *MATLAB Applications for the Practical Engineer.* InTech, 2014, ch. Modeling and Simulation Based Matlab/Simulink of a Strap- Down Inertial Navigation Systems Errors due to the Inertial Sensors.

CHAPTER 2

"Quantifying Errors in Localization Solutions for the Seaglider AUV"

by Wendy Snyder[1], Lora Van Uffelen[2], and Martin Renken[3]

to be submitted to the IEEE Journal of Oceanic Engineering.

[1]Masters Candidate, Department of Ocean Engineering, The University of Rhode Island, Narragansett, RI 02882, Email: wendy_snyder@my.uri.edu

[2]Assistant Professor, Department of Ocean Engineering, The University of Rhode Island, Narragansett, RI 02882

[3]Naval Undersea Warfare Center Division Keyport, Keyport, WA, 98345

Abstract

A Seaglider instrumented with an inertial attitude and heading reference system (AHRS) was tracked for three days on the Dabob Bay acoustic tracking range. Data from the experiment were used to evaluate the accuracy of the Seaglider localization solutions as well as the effects of additional inertial measurements on the accuracy of such solutions. Results showed the localization accuracy of the Seaglider's glide slope model (GSM), with an average horizontal rms error of 12.7 m, was significantly closer to the ground truth than the Seaglider's hydrodynamic model (HDM) which had an average horizontal rms error of 57.9 m. Localization solutions developed using attitude inputs from inertial measurements did not exhibit any statistically significant improvements to the localization accuracy. Sources of error in both of the Seaglider localization models were identified and the magnitude of error resulting from each source was estimated. Results of the analysis were used to develop a modified version of the GSM solution which reduced the average horizontal rms error by 2.9 m resulting in a horizontal rms error metric of 9.8 m. Finally, recommendations for future research were developed based on the results.

2.1 Introduction

The Seaglider autonomous underwater vehicle (AUV) is a small, long endurance, reusable vehicle, capable of collecting oceanographic measurements at a fraction of the cost of an oceanographic research vessel [1]. The Seaglider is commercially available from Kongsberg Underwater Technology Inc. and is primarily used for profiling oceanographic quantities such as temperature, salinity, and oxygen. For these applications, precise vehicle localization is generally not a critical concern. As the glider platform matures, there has been a growing interest in expanding its application and measurement capabilities. One such application is

the use of gliders as moving acoustic receivers in acoustic tomography experiments. This application requires highly accurate localization in order to resolve the fundamental ambiguity between position and sound speed. Errors from hydrodynamic models alone have been estimated to be on the order of 600 – 900 m rms for dives to 1000 m [2]. These errors can be reduced to the order of 80 m rms using position estimates from acoustic tomography source transmissions at long range [3]; however such sources often only transmit every few hours and increase the cost and complexity of deployments. Developing a better understanding of the magnitude and sources of error in the Seaglider localization solutions is an important step in improving localization estimates and expanding the capabilities of the platform.

When a vehicle is underwater, fixes from global positioning systems (GPS) are not available as the GPS signals do not propagate far underwater. Many other types of AUVs rely on inertial navigation systems (INSs) for localization and navigation when underwater for extended periods of time. When aided by a Doppler velocity log (DVL), INSs are capable of achieving position error growth of $\sim$0.2% distance traveled (2σ) [4]; however, a DVL is only capable of operating within a few hundred meters of the seafloor and thus could not be used on a vehicle such as a Seaglider which operates in the mid-water column. Recent work has been done using the *Sirius*, *Sentry*, and *HUGIN* AUVs to improve mid-water localization using velocity estimates of ocean currents from acoustic Doppler current profilers (ADCPs) in place of DVLs, to aid inertial measurement units (IMUs) [4][5][6].

Inertial navigation systems with real-time ocean current velocity measurements have not been used on glider-type AUVs due to the relatively high power requirements of such systems compared to the low power of glider platforms. However, more recent developments in micro-electro-mechanical system (MEMS)-based inertial measurement technology have made integration of inertial measurement

units on glider platforms more feasible. Understanding the potential for improvements to localization from such inertial systems is another important step toward improving localization accuracy for glider platforms.

A tracking experiment and associated data analysis methods to evaluate the localization accuracies for the Seaglider AUV with and without a MEMS IMU are outlined in Section 2.2. A summary of the estimators developed to process inertial data is included in Section 2.3. Section 2.4 presents the results of the tracking experiment and Section 2.5 provides a discussion of the errors in localization results. Section 2.6 uses these results in developing an improved localization solution for the Seaglider. Conclusions and recommendations for future work are in Section 2.7.

2.2 Methods

2.2.1 Dabob Bay Acoustic Tracking Experiment

An experiment was performed on the Dabob Bay acoustic tracking range operated by the Naval Undersea Warfare Center (NUWC) Division Keyport to investigate both the accuracy of the Seaglider's current localization estimates and the effects of incorporating additional inertial measurements on the accuracy of such solutions. A Seaglider was instrumented with its standard sensor package, including the Sparton SP3004D compass, Seabird conductivity and temperature (CT) sail, and Garmin 15H-W GPS receiver, as well as a Lord 3DM-GX5-25 attitude and heading reference system (AHRS), a 1 MHz Nortek Signature1000 ADCP, and a pinger for active acoustic tracking. The AHRS was mounted inside the Seaglider pressure hull along with a Beaglebone Black datalogger used to log the inertial data during testing (Fig. 2.1). The Lord 3DM-GX5-25 is a MEMS device which incorporates measurements from magnetometers, accelerometers, and gyroscopes in all three axes into an Extended Kalman Filter (EKF) to estimate the glider attitude and heading. Raw measurement outputs and a variety of other computed

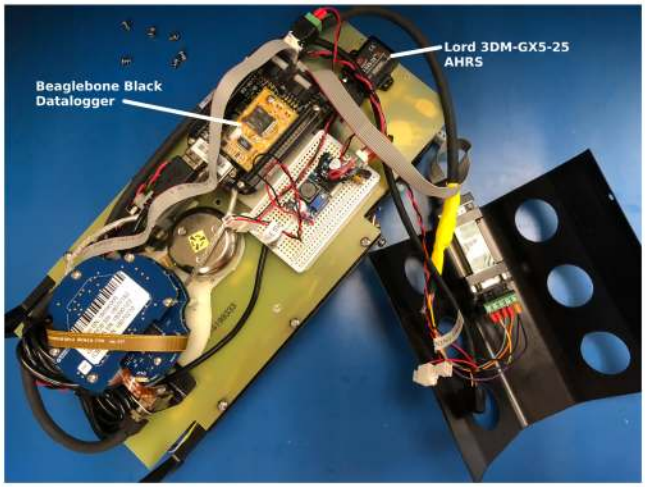

Figure 2.1: Layout of the AHRS and datalogger on the Seaglider during the acoustic tracking experiment on Dabob Bay.

outputs are also available from the sensor. In this manuscript, we will refer to the 'AHRS' when discussing outputs from the built-in EKF on the Lord sensor and the 'IMU' when explicitly referring to the raw inertial data from the Lord sensor. The main advantages of the Lord sensor over the Seaglider's stock compass are the presence of gyroscopes, capabilities of the on-board data processing, and the availability of faster data rates. For this experiment, the AHRS and IMU were both sampled at 10 Hz while the Seaglider compass sampling rate varied throughout each dive depending on processor availability but did not exceed 0.33 Hz. Further details of the sensor selection and integration are outlined in [7].

The Dabob Bay acoustic tracking range is instrumented with a series of short-baseline tracking arrays which were used to actively track the Seaglider during daytime operations. In this work, the acoustic track from the range was assumed to be a ground-truth track from which the accuracy of different localization solutions was evaluated.

During the experiment, the Seaglider was deployed for a total of 68 hours during which time it completed 86 dives. Of these dives, acoustic tracking data

were available for 19 full dives. Due to the bathymetry of the tracking range, dive depths varied between 45 m and 126 m. Of the tracked dives, three of the dives were deemed outliers due to unusual dive dynamics creating unusually high errors. The unusual dive dynamics resulted from an issue with the vehicle's variable buoyancy system and caused the glider to occasionally linger horizontally at the surface for a period of about 10 mins before continuing with the intended dive. These outliers were removed from the data set before computing error metric averages across the set of tracked dives in order to avoid artificially high error estimates.

2.2.2 Range Drift Correction

To maintain accurate ground truth tracking, erroneous fixes were removed from the set of tracking fixes for each dive and a drift correction was applied to the range track data. At the start of the Seaglider deployment, the acoustic pinger used to track the glider was synchronized with the range tracking system. The pinger was then resynchronized ∼45.5 hours into the 68-hour deployment. The resynchronization required a 0.1 sec adjustment to the ping time, indicating a clock drift was present. This drift results from a difference between the assumed 4 sec ping interval and the actual ping interval of the acoustic pinger. From the measured 0.1 sec drift, assuming a constant ping interval, the ping interval error (dt_p) was estimated to be 2.4428e^{-6} sec.

Under the constant ping interval assumption, the error in travel time measured by the range tracking system grows linearly with the number of pings from the time of synchronization. The resulting localization error is then related to this travel time error by the sound speed.

The range (i.e. distance) error (dr) for each ping reception is

$$dr = N_p * dt_p * c_{avg}, \tag{2.1}$$

where N_p is the ping number counted from the most recent synchronization, dt_p is

the ping interval error, and c_{avg} is a harmonic average sound speed computed from range CTD data between the glider depth and array depth for each reception. The estimate of dr was subtracted from the range (i.e. distance) measurement of the raw tracking fix and used with the raw bearing measurement to compute the drift-corrected acoustic tracking location. Neglecting ray bending effects, the bearing angle between the array and pinger is independent of errors in ping interval, as the bearing estimate from the range track solution is based on time difference of arrivals (TDOA) and the travel time error is the same at all hydrophones on the array.

The depth location was corrected using the depth from the Seaglider's on-board pressure sensor which provides more reliable and accurate depth measurements than the acoustic range track.

Ray bending effects were found to be negligible. Assuming the sound speed profile measured by a CTD cast performed during testing, rays corresponding to a variety of different launch angles (measured from the horizontal) were traced from the approximate array depth until they either reached the surface or a horizontal range of 1500 m. A conservative estimate of travel time error of 0.1 sec (the maximum error at the resynchronization time of the pinger) was used to determine the corrected location both by accounting for ray bending and by assuming a straight line path using a harmonic averaged sound speed (Fig. 2.2). The highest errors occurred at shallower launch angles where ray bending is more significant. Without a depth correction, the maximum total error from neglecting ray bending was about 2.3 m. With a depth correction applied, the maximum horizontal range error resulting from neglecting ray bending was 0.25 m, with errors less than 0.01 m at higher launch angles. Additional simulations in which the maximum range was set below 1500 m did occasionally result in slightly higher errors when the track

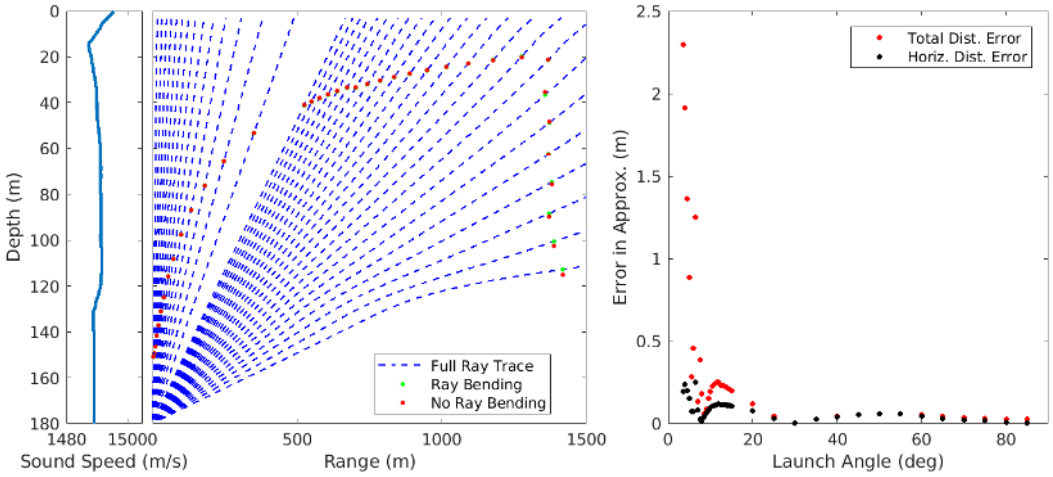

(a) (b)

Figure 2.2: (a) Ray tracing for measured SSP using drift corrected points with and without ray bending. (b) Errors resulting from neglecting ray bending both overall (total dist. error) and correcting for depth (horiz. dist. error only) in the approximated drift correction as a function of the launch angle. A conservative travel time error of 0.1 sec was assumed.

point was near a curve in the ray, but depth corrected errors did not exceed 0.5 m.

To validate the drift correction and initial estimate of ping interval error, drift corrected track estimates were compared to the surface GPS fixes. The range track estimates with ping times closest to the time of the GPS fixes were selected for comparison. Any dives in which the time difference between the GPS fix and range tracking estimate was greater than 10 seconds were not included in analysis to avoid errors resulting from surface drift between the range fix and GPS fix and unrepresentative dives where the start and end of the dive were not tracked.

The minimum average GPS error was 6.5 m which is consistent with the expected accuracy of the GPS fixes obtained by the Seaglider. Average depth errors, computed by comparing the range track estimate of depth with the depth of the Seaglider pressure sensor, were 3.5 to 5 m. These errors could result from tidal variations (2-3 m during the deployment), straight ray assumptions, and

the depth difference between the pressure sensor on the Seaglider and the pinger location.

The ping interval error estimate used for position correction fell between the ping interval errors yielding minimum GPS and depth errors, validating it as an appropriate estimate of the error; the optimal estimate of ping interval error being that which minimizes both GPS and depth errors. Furthermore, because the average GPS error of the drift corrected track solution is within the uncertainty of the GPS unit on the Seaglider, it cannot be determined if the difference between the corrected range track and GPS fix is due to errors in the range track or errors in the GPS fix. The results of this analysis indicate that the corrected range track solution can be used as a reliable ground truth solution for evaluating Seaglider localization accuracy.

2.2.3 Data Analysis Methods

Localization errors were calculated as the distance between the localization estimate and the acoustic range track solution. To quantify and compare the error in the various solutions, a set of error metrics was defined: the maximum error, the root mean square (rms) error, and the normalized maximum error. The maximum error was normalized by the distance traveled throughout the dive, as computed from the range track, to account for the possibility of error scaling with the dive length/duration. The average and standard deviation were computed across all the tracked dives to provide the metric values for each localization solution.

The Seaglider currently has two different localization estimates based on a hydrodynamic model for the vehicle. The solutions are referred to as the glide slope model (GSM) and the hydrodynamic model (HDM). The GSM is the simpler of the two, using attitude measurements and pressure sensor based vertical velocity measurements to estimate the vehicle glide slope and horizontal speed. The HDM

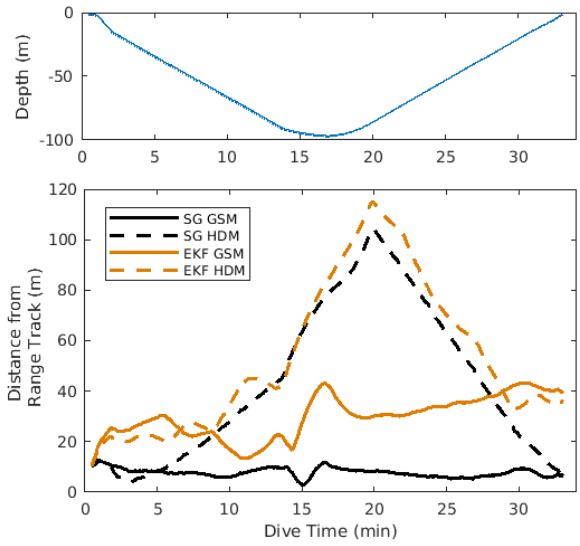

Figure 2.3: Depth vs time (upper) and distance of selected solutions from the acoustic ground truth range track (lower) for Dive 69. Solutions compare GSM results (solid) to HDM results (dashed) and used attitude inputs from the stock Seaglider compass (black) and the AHRS built-in EKF (orange).

incorporates additional temperature and salinity measurements as well as information from the variable buoyancy system to account for the vehicle buoyancy when estimating glide slope, dynamic pressure, and horizontal speed. Both models then dead-reckon using the derived estimates of horizontal speed along with heading measurements and GPS fixes to get the desired localization estimates [1] [7].

Preliminary results from the experiment were presented in [7] and focused on quantifying errors in the standard Seaglider GSM and HDM using attitude inputs from the Seaglider's stock compass (SG) and from the AHRS. Results using the stock compass as the attitude input are referred to as 'SG GSM' and 'SG HDM', while solutions using AHRS attitude estimates are labeled 'EKF GSM' and 'EKF HDM'. The results for a representative dive are shown in Fig. 2.3 and the overall averaged error metrics are given in Table 2.1.

The GSM solutions were more accurate and performed more consistently than the HDM solutions. When attitude estimates from the AHRS were used in the

Table 2.1
Average Error Metrics (with 1σ standard deviation)

	Max Error (m)	RMS Error (m)	Norm. Max Error (%)
SG			
GSM	21.6 (5.6)	12.7 (3.5)	4.3 (1.9)
HDM	103.8 (33.4)	57.9 (17.4)	19.1 (3.6)
AHRS EKF			
GSM	52.6 (26.4)	32.9 (16.4)	9.4 (3.8)
HDM	112.6 (32.9)	66.7 (21.1)	21.0 (3.9)

Seaglider GSM, all error metrics and standard deviation values were more than double those for the GSM using the stock compass. Because of the poor performance of measurements from the AHRS, additional attitude estimates were determined using the raw inertial data from the IMU.

2.3 Inertial Attitude Estimators

Attitude measurements were computed from the raw inertial measurements recorded from the IMU as an alternative to the AHRS's 'black box' built-in EKF. Inertial measurements were recorded at 10 Hz and included raw magnetometer, accelerometer, and gyroscope measurements as well as ΔV and $\Delta\Theta$ measurements, which represent the change in velocity and change in attitude angle, respectively, over the measurement interval. The ΔV and $\Delta\Theta$ measurements are each generated by summing up 100 accelerometer and gyroscope measurements within a 0.1 s sample interval, and are essentially short-time averaged acceleration and angular rate measurements to reduce white noise. To convert these measurements to acceleration and angular rate units they must be divided by the length of the sample interval (0.1 s).

Three different inertial attitude estimators are described in the subsequent sections. A tilt compass style attitude estimator which relies solely on accelerometer

and magnetometer data from the IMU is described in Section 2.3.1. An overview of a threshold attitude estimator which incorporates accelerometer, magnetometer, and gyroscope measurements from the IMU is provided in Section 2.3.2. Finally a custom Kalman filter estimator which aims to optimally weight measurements from all accelerometers, magnetometers, and gyroscopes on the IMU is described in Section 2.3.3. For the remaining analysis, we will focus on the GSM solution as it was significantly more accurate and reliable in estimating dive trajectories than the HDM solution.

2.3.1 Tilt Attitude

To get a baseline comparison between the stock compass and the IMU, a tilt attitude solution from the IMU data was developed utilizing the same attitude estimation methods as the Seaglider currently uses for the stock compass data. The tilt attitude solution used the ΔV measurements from the IMU divided by the sampling interval in place of accelerometer measurements, as ΔV measurements are less noisy than accelerometer measurements.

For the purposes of this manuscript, we define a body frame, b, in which the x axis points forward along the central (roll) axis of the vehicle, the y axis points to the right of the central axis and aligns with the pitch axis of the vehicle, and the z axis completes the orthogonal set pointing down (Fig. 2.4). The local navigation frame, n, is defined such that the origin is located at the body frame origin, the x axis points toward true north, the y axis points toward true east and the z axis aligns with the gravity vector pointing down.

Under the assumption that no linear vehicle accelerations are present, accelerometers measure only the acceleration due to gravity. Attitude estimates for pitch and roll are then determined by fitting the measured accelerometer vector to the known gravity vector in a technique known as leveling. The leveling equations

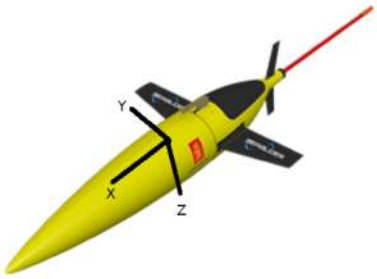

Figure 2.4: Definition of the body coordinate frame

are expressed as

$$\phi = \arctan 2\left(-f_y^b, -f_z^b\right) \tag{2.2}$$

$$\theta = \arctan\left(\frac{-f_x^b}{\sqrt{(f_y^b)^2 + (f_z^b)^2}}\right) \tag{2.3}$$

where $\arctan 2$ is the four-quadrant inverse tangent function, ϕ is the roll angle, θ is the pitch angle, and $\mathbf{f}^b$ (sometimes expressed $\mathbf{f}_{ib}^b$) is the vector of specific force measured by the accelerometers expressed in the body frame where subscripts indicate the x, y, and z directional components [8].

Assuming no magnetic disturbances, the IMU magnetometers measure the Earth's magnetic field. The Earth's magnetic field vector varies in location and time, but over the short duration and small area of the Seaglider deployment the magnetic field was assumed constant and determined using the World Magnetic Model (WMM) [8].

To determine the vehicle heading, the magnetic field strength measured by the magnetometers was rotated according to the pitch and roll of the vehicle and fit to Earth's known magnetic field vector. The magnetic field vector as measured by the magnetometer in the body frame ($\mathbf{h}^b$) was rotated into the local navigation frame ($\mathbf{h}^n$) using

$$\mathbf{h}^n = \mathbf{C}_b^n(\phi, \theta, \psi = 0)\mathbf{h}^b, \tag{2.4}$$

where $\mathbf{C}_b^n(\phi, \theta, \psi = 0)$ represents a direction cosine matrix (DCM, also called a

rotation matrix) from the body frame to the local navigation frame with inputs for roll and pitch only (i.e. assuming a heading of zero) [9]. The magnetic heading (ψ_m^b) is given as,

$$\psi_m^b = -\arctan 2\left(h_y^n, h_x^n\right), \tag{2.5}$$

where h_x^n and h_y^n are the x and y components of the measured magnetic field vector in the local navigation frame. The magnetic heading angle is referenced to the direction of magnetic north at the location of the measurement rather than geographical (or true) north. The magnetic variation at the location of the measurement is added to the magnetic heading to reference to true north [8]. Similar to the leveling technique, magnetometer based headings are most accurate under low acceleration conditions and when no magnetic disturbances are present.

From (2.2), (2.3), (2.4), and (2.5) a complete attitude estimate for the Seaglider can be determined solely using the raw accelerometer and magnetometer measurements from the IMU. Results using attitude estimates from this algorithm are labeled as 'Tilt' in the results.

While the magnitude of the measured magnetic field should remain constant and equal to the magnitude of Earth's magnetic field at the location of the measurement, the strength of the measured magnetic field was observed to vary with the pitch of the vehicle (Fig. 2.5). This indicated that the IMU was affected by the magnetic field of the battery which acts as a mass shifter in the Seaglider. The stock compass, which was mounted farther from the electronics and battery pack, did not seem to be affected by these interferences and was able to be calibrated.

The presence of a magnetic disturbance was verified in a lab experiment. The Seaglider was laid in a neutral pitch and roll position and the sensor was secured on top of the vehicle's outer fairing at various distances from the main battery. For each mounting location, the battery was moved through its full range of motion

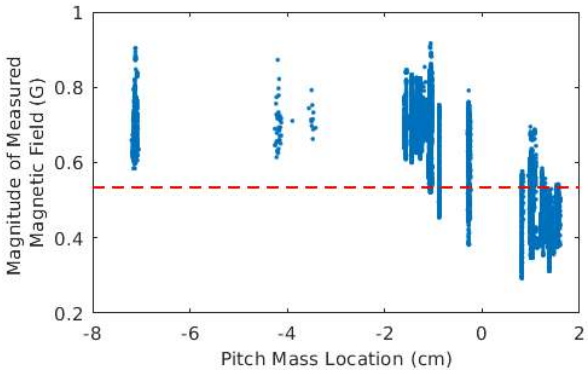

Figure 2.5: Comparison of measured magnetic field strength for the IMU magnetometers to the location of the pitch mass in the Seaglider. Negative locations are closer to the sensor. When the pitch mass (battery) is closer to the IMU (negative location), the measured magnetic field is larger than expected for Earth's field at that location (0.534 Gauss marked by the red line).

while measurements were logged from the IMU. The closer the sensor was mounted to the battery, the larger the variation in the heading estimate from the sensor. When the sensor was mounted ∼59 cm from the closest point of the battery's range of motion, heading varied less than 1 deg through the entire range of battery motion. However, when moved ∼8 cm from the battery, heading variation exceeded 20 deg through the range of battery motion. For the Dabob bay experiment, the IMU was mounted about 36 cm from the battery. When mounted at this distance in the lab, heading variations of 2 – 3 deg were measured.

To eliminate concerns of magnetic interference, a second solution which combined raw magnetometer measurements from the stock compass with the IMU accelerometer measurements using the tilt attitude equations was investigated. This solution, referred to as 'Tilt (Stk mag)', reduces effects of the magnetic disturbance on heading estimate, however it does introduce additional questions concerning sensor alignment.

2.3.2 Threshold Attitude

With the exception of data rate, the main difference between the stock compass and the IMU is the availability of gyroscope measurements from the IMU. To determine the effects of the gyroscope measurements on the solution accuracy, additional attitude estimates were made using the full set of measurements from the IMU. One relatively simple attitude integration algorithm uses thresholds to determine whether to rely on accelerometer or gyroscope measurements for attitude at each data point. The algorithm flowchart is shown in Fig. 2.6.

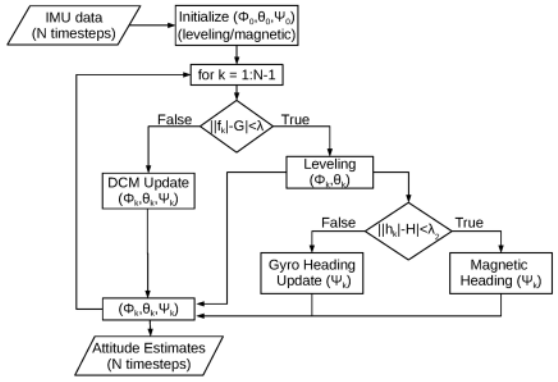

Figure 2.6: Threshold Algorithm Flowchart

Inputs to the algorithm consist of the raw IMU data including accelerometer (ΔV), gyroscope ($\Delta\Theta$), and magnetometer measurements. In order to compute any attitude updates using the gyroscope measurements, attitude estimates must first be initialized. Leveling and magnetic heading equations [(2.2), (2.3), (2.4), and (2.5)] were used on the first set of data points to provide an initial attitude estimate. The algorithm loops through each set of measurements and determines an attitude estimate for each time step. Since leveling is most reliable in the absence of linear acceleration, the algorithm first attempts to detect any linear acceleration present by comparing the magnitude of the measured acceleration

vector ($|\mathbf{f}|$) to the known magnitude of gravitational acceleration (G = 1 g $\approx$ 9.81 m/s^2). If the difference between the measured magnitude and the expected magnitude is larger than a selected threshold (λ = 0.01 g), linear acceleration is present. The attitude expressed as Euler angles (roll, pitch, and yaw) is converted to a DCM, then updated from the measured $\Delta\Theta$ values using the DCM update equation

$$\mathbf{C}_b^n(t+\tau) = \mathbf{C}_b^n(t)\left(\mathbf{I}_3 + \frac{\sin|\boldsymbol{\alpha}_{ib}^b|}{|\boldsymbol{\alpha}_{ib}^b|}[\boldsymbol{\alpha}_{ib}^b\wedge] + \frac{1-\cos|\boldsymbol{\alpha}_{ib}^b|}{|\boldsymbol{\alpha}_{ib}^b|^2}[\boldsymbol{\alpha}_{ib}^b\wedge]^2\right), \tag{2.6}$$

where $\mathbf{C}_b^n$ (shorthand for $\mathbf{C}_b^n(\phi,\theta,\psi)$) is the DCM matrix used to rotate vectors between the body and local navigation frame, τ is the time step between gyroscope samples, $\boldsymbol{\alpha}_{ib}^b$ is the vector of attitude increments over the time step ($\Delta\Theta$ measurements), and $[\boldsymbol{\alpha}_{ib}^b\wedge]$ represents a skew-symmetric matrix of attitude increments [8]. If the acceleration difference does not exceed the threshold (λ), leveling equations (2.2) and (2.3) determine the roll and pitch angles from accelerometer measurements.

Magnetic headings are most reliable in the absence of both linear acceleration and magnetic disturbance [8]. In the case where linear accelerations are detected, the heading is also updated as part of the DCM update. However, if no linear acceleration is detected, the algorithm compares the magnitude of the measured magnetic field ($|\mathbf{h}|$) to the expected magnetic field magnitude (H = 0.534 Gauss), based on the WMM for the Dabob Bay region. If the difference between the measured magnetic field strength exceeds a certain threshold (λ_2 = 0.05 Gauss), a magnetic disturbance is considered present and $\Delta\Theta$ measurements are used to update the heading estimate according to

$$\psi(t+\tau) = \psi(t) + (\sin\phi\sec\theta)\alpha_y + (\cos\phi\sec\theta)\alpha_z, \tag{2.7}$$

where $\psi(t)$ is the heading at the previous time step t [10]. If a magnetic disturbance is not detected, the heading is updated using the magnetometer data in (2.4) and

(2.5). Each iteration of the loop outputs a set of attitude measurements based on raw IMU measurements during that time step.

For each dive, the threshold method was first used to generate attitude estimates using raw measurements from the IMU. Solutions using these attitude estimates are labeled as 'Thresh' in the results. Then a second set of attitude estimates, referred to in results as 'Thresh (Stk mag)', was generated using raw inertial measurements from the IMU and magnetometer measurements from the stock compass to remove effects of the magnetic disturbance. Since the stock compass had a slower time-varying sample rate, the gyroscope-based heading update was applied at time steps where magnetometer measurements were not available.

2.3.3 Custom Kalman Filter

A Kalman filter (KF) was also developed to estimate the Seaglider attitude based on inertial measurements from the IMU. Solutions using attitudes from this estimator are labeled as 'KF' in the results. Unlike the threshold method in which each time step uses either gyroscope or accelerometer measurements exclusively, the Kalman filter uses all available measurements to estimate the attitude at each time step. The custom Kalman filter was based on a simplified version of the adaptive Kalman filter for MEMS-IMU and magnetometer integrated AHRS developed by Li and Wang in [9]. The model proposed by Li and Wang avoids the nonlinearity problems present in many other AHRS Kalman filter models and reduces unwanted effects resulting from dynamic accelerations. Additionally, it was specifically developed considering low-cost/low-accuracy MEMS-type IMUs making it a good option for the Seaglider application.

There were two main simplifications applied to the model outlined by Li and Wang for this application. First, the gyroscope scale factor estimates were removed

from the state vector leaving the resulting state vector ($\mathbf{X}$) as

$$\mathbf{X} = [\Psi_N, \Psi_E, \Psi_D, G_{bx}, G_{by}, G_{bz}]^T \tag{2.8}$$

where Ψ_N, Ψ_E, and Ψ_D represent attitude errors between the computed navigation frame (n_c) based on the IMU and the true navigation frame (n), and G_{bx}, G_{by}, and G_{bz} are the constant bias in the gyroscope measurements in the body frame. The second simplification was applied to the system matrix ($\mathbf{F}$). Because of the slow speed of the Seaglider ($\sim$20 cm/s) and the relatively high noise characteristics of the gyroscopes, the rotation rate of the navigation frame with respect to the inertial frame was assumed to be zero. The resulting system matrix is

$$\mathbf{F} = \begin{bmatrix} \mathbf{0}_3 & -C_b^{n_c} \\ \mathbf{0}_3 & \mathbf{0}_3 \end{bmatrix} \tag{2.9}$$

where $C_b^{n_c}$ is a rotation matrix between the body frame and the computed local navigation frame and $\mathbf{0}_3$ represents a 3-by-3 zero matrix.

After each iteration of the Kalman filter, estimated errors in the state vector were fed back into the DCM update (2.6) to correct the gyroscope-based attitude, creating a closed-loop filter. Since error estimates were fed back into the solution, the state vector was reset to zero after each iteration, simplifying the Kalman filter update equations. The closed-loop implementation also ensures error states remain small maintaining stability of the filter solution [8].

The Kalman filter also incorporates a dynamic acceleration detection similar to that used in the threshold estimator. If the magnitude of the measured acceleration differs from the expected acceleration due to gravity by more than a given threshold (0.01 g), the Kalman gain is set to zero causing accelerometer and magnetometer measurements to effectively be ignored. The value of the threshold was estimated based on the expected magnitude of the accelerometer noise and refined in tuning of the Kalman filter.

A modified version of the Kalman filter was also developed to combine magnetometer measurements from the stock compass with the IMU inertial measurements, as done for the other attitude estimators. The modified Kalman filter included the heading innovation measurement when magnetometer measurements were available and relied on gyroscope-updated heading at time steps where the magnetometer measurements were not available. Solutions using attitude estimates from this alternative Kalman filter are labeled as 'KF (Stk mag)' in the results.

2.4 Results

2.4.1 Localization Solutions

For each of the attitude estimators described in Section 2.3, the resulting attitude estimates were used as inputs to the Seaglider GSM solution to generate localization solutions for each dive. The estimated dive trajectories were then evaluated against the ground truth track from the Dabob Bay tracking range. While there was significant variability across different dives, Fig. 2.7 shows some of the observed trends. The threshold method with IMU magnetometer data, generally had much higher error across all dives. The Kalman filter using the IMU magnetometers was generally extremely close to the Tilt solution that used the IMU magnetometers. Additionally, the solutions using the stock compass magnetometers (dashed and labeled '(Stk mag)') had slightly lower error than those using the IMU magnetometer data.

The error metric values of the individual tracked dives for a select set of solutions are shown in Fig. 2.8 and the averaged values of the metrics for all GSM solutions are listed in Table 2.2 along with their 1σ standard deviations. Solutions using the IMU inertial measurements all generally had higher errors than the Seaglider's standard GSM solution using the stock compass.

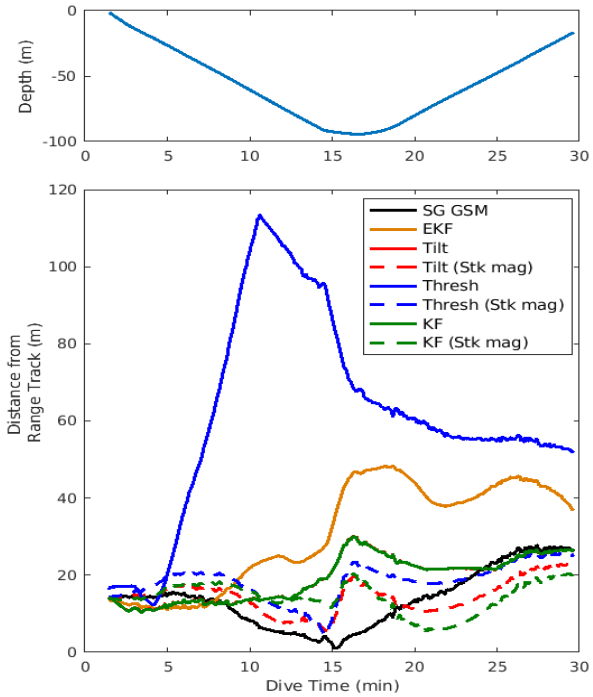

Figure 2.7: Depth vs time (upper) and distance of all GSM solutions from the acoustic ground truth range track (lower) for Dive 57. Solutions were all generated from the GSM using attitude inputs from: the Seaglider's stock compass (black), the AHRS built-in EKF (orange), the tilt attitude estimator using IMU measurements (red), the threshold attitude estimator using IMU measurements (blue), and the custom Kalman filter using IMU measurements (green). Solutions using the stock compass magnetometer data with IMU inertial data (dashed) are labeled as '(Stk mag)'. Results of the Tilt and KF solutions were so close the lines are nearly on top of each other.

The error metrics for the solution using the built-in EKF generally increase with dive number which may result from drift in the EKF solution. The first few tracked dives (Dives 1, 2 and 4) were just after the filter initialized and rms error was 9 m on average. After the filter had been running for over 24 hours, the later set of tracked dives (Dives 57 to 69) had rms errors ranging between 23 m and 67 m with an average dive rms error of 38 m. Such growth in error could result from a poorly tuned EKF in which uncertainty of the attitude estimates is improperly estimated by the filter solution to be lower than the measurement uncertainties.

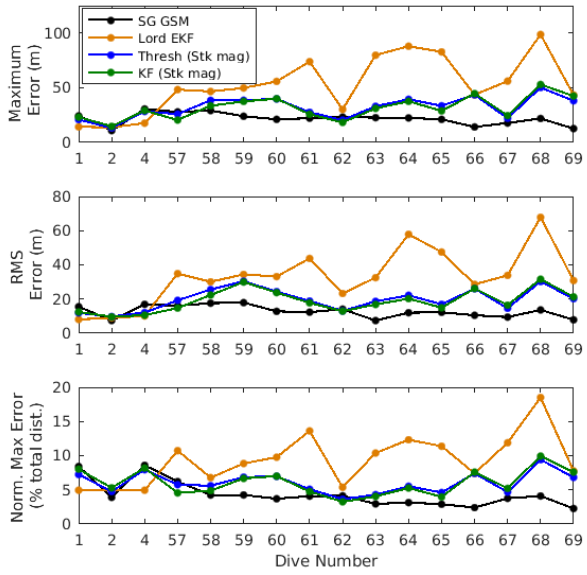

Figure 2.8: Error metric values for each tracked dive and a select set of attitude solutions using the GSM. Solutions used attitude inputs from: the Seaglider's stock compass (black), the AHRS built-in EKF (orange), the threshold attitude estimator using IMU inertial measurements with the stock compass magnetometers (blue) and the custom Kalman filter using IMU inertial measurements with the stock compass magnetometers (green).

In this condition, the EKF will rely less on measurement data to correct state estimates leading to a divergence of the estimated attitude from the true attitude.

The increased error in the threshold estimates using the IMU magnetometer is most likely due to the apparent magnetic disturbances present in the IMU magnetometer data. In the presence of magnetic disturbances, the heading solution relies on gyroscope integration which can cause the heading estimate to drift rapidly from the true value due to the integration of measurement noise. These effects are typically constrained by frequent independent magnetic heading updates. In the case of the threshold estimator, the magnetic disturbances caused about 77% of all magnetometer measurements to exceed the threshold of the magnetic disturbance detector with the percent per dive varying between 56% and 100% of measurements. This significantly limited the frequency of magnetic heading

Table 2.2
GSM Average Error Metrics (with 1σ standard deviation)

	Max Error (m)	RMS Error (m)	Norm. Max Error (%)
SG GSM	21.6 (5.6)	12.7 (3.5)	4.3 (1.9)
Tilt			
w/ IMU Mag	35.2 (9.8)	21.5 (6.7)	6.8 (2.0)
w/ Stock Mag	33.0 (10.4)	19.8 (6.9)	6.2 (1.7)
Thresh			
w/ IMU Mag	82.8 (56.7)	51.5 (33.2)	16.8 (12.9)
w/ Stock Mag	31.9 (9.9)	19.5 (6.5)	6.0 (1.5)
KF			
w/ IMU Mag	35.3 (9.8)	21.5 (6.6)	6.9 (2.0)
w/ Stock Mag	31.5 (10.5)	18.8 (6.6)	6.0 (1.9)

updates. As the errors in the heading increase, so do errors in the localization solution leading to the large errors observed in the threshold method when IMU magnetometers were used.

The Seaglider's current GSM solution has the lowest value for all error metrics. The attitude solutions from the IMU suffered from imprecise alignment of the IMU which is addressed further in Section 2.5.2, but given the results here is not expected to have improved localization accuracy.

To compare the effects of the additional gyroscope measurements on the localization accuracy, the tilt attitude GSM was considered a baseline solution for the IMU, as the tilt solution uses the same types of measurements and estimation equations as the stock Seaglider solution. Compared to this tilt baseline, the results of the threshold and custom Kalman filter GSM solutions do not show statistically significant reductions in the error. This indicates that the introduction of additional measurements from the gyroscope does not have a significant effect on the accuracy of the localization solution for the short, shallow dives performed in this experiment.

2.4.2 Error Simulation

To determine the expected magnitude of errors due to noisy attitude estimates, a simple simulation was developed. A set of "true" attitude angles was generated based on an idealized Seaglider dive and used as inputs to the GSM to determine the localization solution assuming no errors in the model. Inertial measurements for the compasses were generated from the true attitudes with noise simulated according to sensor specifications. The noisy measurements were fed back into attitude estimators and ultimately the GSM. Comparing the output of the GSM solution using the "true" attitudes to that using the noisy attitudes gave an estimate of the error resulting from noisy attitude measurements.

To consider effects of sensor misalignments, the simulation was repeated adding 1 deg of error to the pitch and heading before they were input into the model. Results from the simulation of a 90 m dive similar to those performed during the Dabob Bay experiment are shown in Fig. 2.9.

Over the 90 m simulated dive, the noise from the stock compass resulted in a maximum error of 0.94 m and a rms error of 0.33 m. The noise from the IMU resulted in a maximum error of 0.88 m and a rms error of 0.26 m. The introduction of misalignment significantly increased these errors, with 1 deg of pitch offset resulting in a maximum error of 10.6 m and a rms error of 5.1 m and 1 deg of heading offset resulting in a maximum error of 2.4 m and a rms error of 1.2 m. The significant increase in error with pitch offset is likely due to the model dependence on pitch to compute horizontal speed.

2.4.3 Model Analysis

Velocities and glide slope angle, intermediate outputs of the GSM and HDM models, were compared to estimates of the parameters computed from the range data and vehicle pressure sensor. Estimates from the acoustic range track were

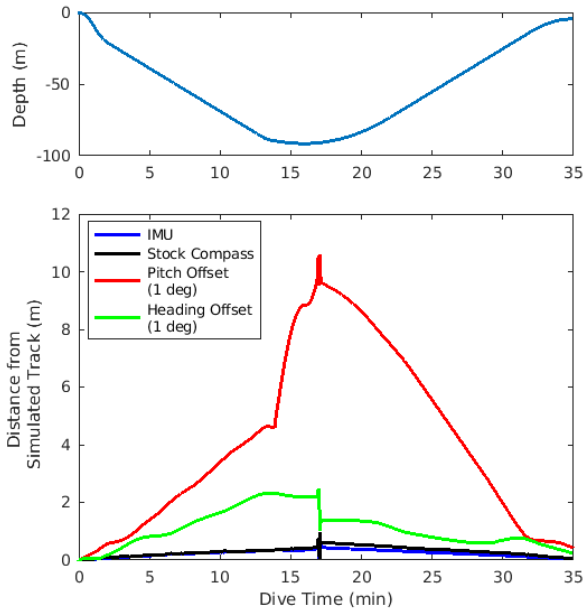

Figure 2.9: Simulated errors resulting from noisy attitude inputs to the Sealider GSM localization solution. Noisy inertial measurements and magnetic measurements were generated by adding simulated noise according to sensor specifications for the IMU (blue) and stock compass (black). Attitude estimates generated from the noisy data were used as model inputs. Misalignment errors were also added to the estimates to simulate errors due to pitch misalignment (red) and heading misalignment (green). Depth vs time (upper) and the difference between the GSM output using the noisy attitudes and the GSM output using 'known' attitude plotted as a function of dive time (lower).

smoothed to reduce noise. The results for a representative dive are shown in Fig. 2.10.

The HDM and GSM solutions had similar estimates of glide slope except at the start of the dive and near apogee. During regions of agreement between the models, the estimates of glide slope were typically within 5 deg of those estimated from the range data which was considered consistent given the relatively noisy range estimates. There was however, a noticeable discrepancy between the GSM and HDM horizontal speed estimates throughout a significant portion of the dive typically on the order of 5 – 15 cm/s. The horizontal speed of the GSM was much

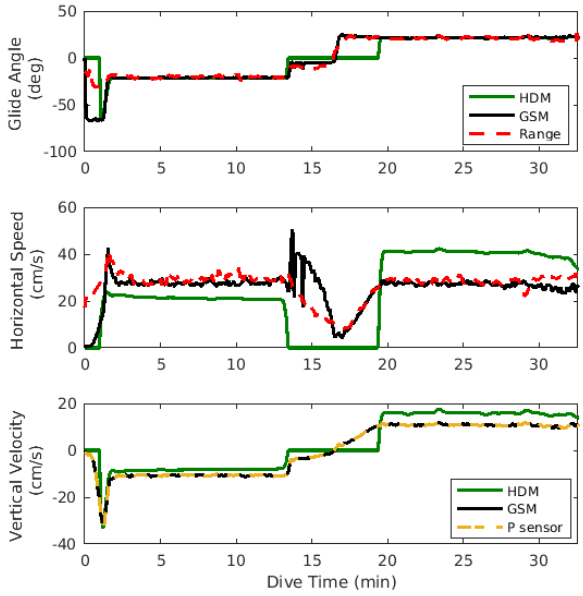

Figure 2.10: Comparison of intermediate parameter values in the GSM (black) and HDM (green) solutions using the Seaglider's stock compass to parameter values estimated from the range track (red) for Dive 69. The vertical velocity estimate (3rd panel) shows the estimate generated by the pressure sensor measurements (yellow) instead of from the range data.

closer to the horizontal speed determined from the range track than the HDM model, except at the very start of the dive. The vertical velocity output by the HDM solution also typically differed from the depth rate of change based on the pressure sensor on the order of 2 – 6 cm/s. While the vertical velocity is not used directly in the dead-reckoned solution, the discrepancy in vertical velocity is also indicative of an error with the overall HDM speed estimate from which the horizontal speed and vertical velocity are derived.

2.5 Discussion of Sources of Error

Errors in the localization solutions considered here come from a variety of sources such as uncertainty in GPS fixes, errors in attitude measurements, and errors in the model itself. Additionally, there is a small amount of uncertainty in

the ground truth track used to estimate the localization errors.

2.5.1 Sources of Error in the HDM

In the HDM solution, the primary source of error resulted from an error in the model's estimate of horizontal speed. The horizontal speed estimated by the HDM differed from the GSM and range estimates on the order of 5–15 cm/s (Fig. 2.10, panel 2), slower during dive and faster during climb. A speed error of 10 cm/s over the first 15 min of a 30 min dive, would result in 90 m error. This estimated maximum error magnitude is comparable to that measured for the HDM localization solution (Table 2.1), indicating much of the measured error is likely due to a speed discrepancy. Furthermore, the change in direction of the offset is consistent with the growth then decay of error as measured for the HDM solution (Figure 2.3).

At the start of the dive and near apogee, poor flow through the conductivity sensor caused some conductivity measurements to be erroneous and disregarded resulting in a default buoyancy value of zero. These data points of zero buoyancy, when processed by the HDM, yielded speeds and thus displacements of zero. In most cases where this occurred, a speed of zero was an unreasonable assumption and not consistent with the range track data. While the errors due to bad conductivity measurements were likely small compared to the overall error in the HDM solution, correcting erroneous conductivity measurements with interpolated values or some other default buoyancy value would improve the model.

2.5.2 Sources of Error in the GSM

Errors in the GSM model were more difficult to pinpoint as the total error was smaller than that of the HDM. The three main sources of error considered were errors in attitude estimates, model errors, and errors due to GPS fixes and surface drift.

Attitude Measurement Errors

Overall, the stock compass measurements performed better in the GSM localization solution than those from the IMU and AHRS. Sensor misalignment and magnetic disturbances are believed to be the main reasons for the performance difference.

On average, the pitch estimates between the stock compass and IMU were offset by 1.6 deg. As the stock compass is established as part of the Seaglider design, the mounting and alignment of the sensor is likely more precise than the alignment of the newly integrated Lord sensor. Additionally, results using the stock compass attitudes provided lower error metrics. The stock compass was therefore assumed to be the accurate measure of pitch when correcting for the misalignment of the IMU. When the 1.6 deg offset was removed from the IMU attitude estimates and the undisturbed magnetometer measurements were used (Stk mag), the resulting error metrics approached those of the stock compass GSM solution (Table 2.3). This indicated mounting misalignment was a significant factor in the performance discrepancy between the two sensors. The effects of misalignment were further confirmed from the results of the simulation (Fig. 2.9).

Table 2.3
GSM Average Error Metrics Using Corrected Pitch Alignment
(with 1σ standard deviation)

	Max Error (m)	RMS Error (m)	Norm. Max Error (%)
SG GSM	21.6 (5.6)	12.7 (3.5)	4.3 (1.9)
Tilt (Stk mag)	23.6 (5.9)	14.2 (3.1)	4.7 (2.1)
Thresh (Stk mag)	23.4 (6.6)	14.3 (3.4)	4.7 (2.2)
KF (Stk mag)	22.4 (4.7)	13.5 (2.7)	4.5 (1.8)

While Fig. 2.9 indicated sensor misalignment can have significant effects on the output of the GSM solution, attitude noise also introduced some errors into the

solution; however, the lower noise of the IMU compared to the stock compass had an almost negligible reduction in error resulting from noise alone, indicating that reducing noise in the attitude solution is not as critical to localization accuracy as ensuring proper alignment and improving the model itself. The negligible effect of reducing noise in attitude is also consistent with the results of Table 2.3.

Another factor affecting attitude estimates is magnetic disturbance. The mounting location of the IMU was closer to the electronics and battery pack of the Seaglider than the stock compass, where it was more prone to magnetic field interference (Fig. 2.5). Careful mounting of the sensor and calibrating for (or avoiding) magnetic interference would most likely provide further improvements in the accuracy of the localization solutions using data from the IMU.

Model Errors

One common trend in the GSM solutions was a rapid increase in error near the apogee point of the dive (near minute 15 of Fig. 2.7). These error spikes were accompanied by a spike in horizontal speed near apogee which were not consistent with speed estimates from the range track (Fig. 2.10). The GSM largely relies on the assumption that the Seaglider moves along a path at a set glide slope and heading. The vertical velocity is then used to estimate horizontal speed; however, near apogee the glider approaches a nearly horizontal pitch. Under the model assumptions, a large horizontal speed is required to compensate for even very slow vertical velocities at these small glide slopes. At a glide slope of zero, a singularity occurs and the horizontal speed goes to infinity. In reality, at this point in the dive, the vertical motion is independent of horizontal speed. As the vehicle begins to pitch upward and pump oil to achieve positive buoyancy it may continue to sink or begin to float (depending on its relative buoyancy) independent of forward glide motion.

During this region of near neutral pitch, the horizontal speed estimated from the range track was observed to decrease almost linearly, independent of vertical velocity. Under the current GSM solution, there is a "stall condition" where horizontal speed is assumed to be zero if the horizontal speed estimate exceeds 100 cm/s and the glide slope is less than 5 deg. No other compensations are made to accommodate the different dive dynamics likely occurring at this point in the dive. Additionally, because of the rapid change in speed with angle, slight pitch errors at this point in the dive create more significant speed–and thus position–errors than at other points in the dive. To correct for such errors in the future, more must be understood about the vehicle dynamics at apogee.

GPS Error

Based on a comparison of multiple GPS fixes from a stationary Seaglider, uncertainties in the GPS fixes were estimated to be on the order of a few meters, with maximum errors of 7 to 10 m. Additionally there is typically about a minute between the starting GPS fix at the beginning of the dive and the first vehicle data for computing displacements and often over two minutes between the last computed displacement and the final GPS fix at the end of the dive. During these gaps in data collection the vehicle is most likely drifting at or near the surface, but the model assumes it is stationary. Depending on surface currents, this has the potential to introduce further error into the localization solutions. Such error may also compound between the start and end of the dive resulting in larger depth averaged current estimates.

The range track was used to correct the dive start and end location inputs to the GSM solution. The range track point closest in time to the start and end attitude measurements from the glider were used as start and end locations. The use of the range track in this way removes effects from the GPS errors, surface

drift, as well as any slowly-varying offsets in the range track.

When start and end locations were corrected in the GSM solution using various attitude estimates, the maximum error metric improved in all cases by 2.5 – 4 m and the rms error was improved by 3.5 – 5 m.

Summary of GSM Errors

It is estimated that for the 90 m dives completed during the Dabob Bay experiment the GPS and surface drift errors accounted for about 27% of the rms error in the GSM solution while noise in attitude estimates accounted for about 3% of the rms error. The remaining 70% of the rms error is from other model errors, sensor calibration and alignment errors, as well as any other unconsidered effects.

These error percentages are not assumed to hold for a full depth dive to 1000 m. The GPS error ($\sim$4 m rms) is expected to remain fairly constant regardless of dive depth causing the percentage of error due to GPS to decrease as total error increases. The errors due to the attitude and the model are expected to grow with increasing dive depth. While the growth of attitude errors with depth could be estimated from simulations of deeper dives, growth of model errors and other sources are difficult to estimate without additional knowledge or data.

2.6 Development of a Modified GSM

Based on the results of the error analyses, a modified version of the glide slope model was developed (referred to as 'mod GSM' in results). The modified GSM sought to correct two identified sources of error in the original solution: the horizontal speed estimate at apogee and the surface drift at the start and end of the dive.

The horizontal speed estimates from the range track for all tracked dives con-

sistently indicated the Seaglider decelerated linearly throughout the apogee phase of the dive. The modified GSM solution improves the horizontal speed estimate during apogee by assuming a linear deceleration between the speed estimates just before and just after apogee. Figure 2.11a shows an example of this correction applied to a dive from Dabob Bay. The apogee phase of the dive is determined from the pitch angle of the glider as marked in orange on the upper plot. Trends in the horizontal speed estimates (lower plot) were consistent across all tracked dives and indicated the modified GSM estimates fit more closely with the range data than the standard GSM solution.

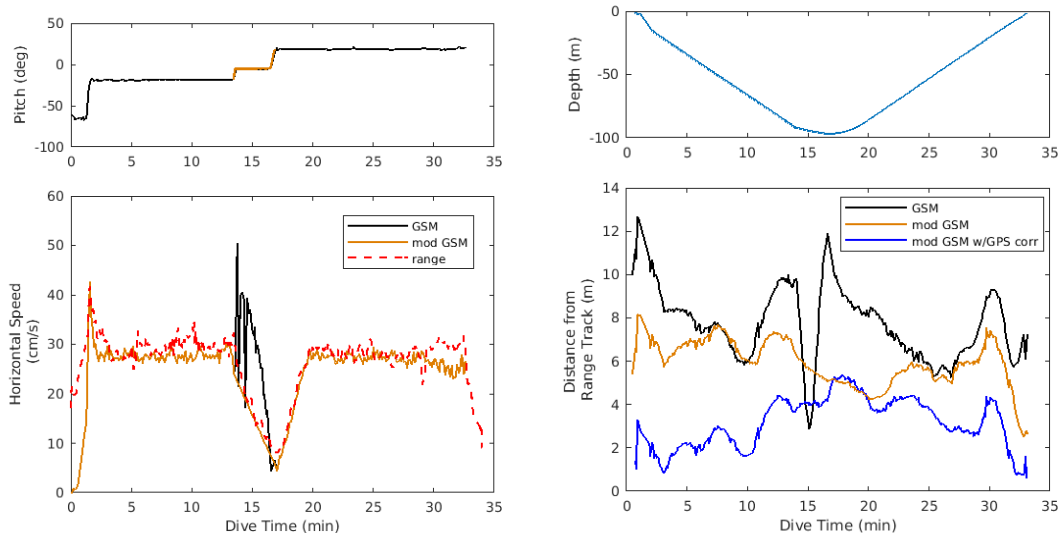

(a) Speed Correction

(b) Error Analysis

Figure 2.11: Dive 69: (a) Pitch angle through the dive with region of speed correction marked in orange (upper). Comparison of horizontal speed estimates from the GSM and modified GSM to the estimate from the range data (lower). (b) Depth vs time (upper). Localization solution distance from the range track for the standard GSM (black), modified GSM (orange), and modified GSM with GPS correction (blue) solutions.

The second correction applied accounts for surface drift during the gaps between when the Seaglider achieves a GPS fix and the start and end of the dive. The

Seaglider estimates a surface current based on the distance it travels between the surfacing GPS fix and the GPS fix just before the start of the dive. The correction assumes a constant velocity drift between the time of the GPS fix just before diving and the first dive data recorded by the Seaglider. A similar correction was applied at the end of the dive from the time of the last dive data recorded until the first new GPS fix is achieved. Since on deep dives the Seaglider surfaces hours after it started and often more than a kilometer or two from the starting location, the same surface drift estimate is most likely not valid upon resurfacing. Thus, if data from the following dive are available, the surface current upon surfacing is taken from the subsequent dive file where additional GPS data are available. The impact of surface current correction on localization is dependent on the magnitude and variability of surface currents in the region of deployment. Additionally, estimates of surface currents depend highly on GPS fixes and are subject to the effects of GPS uncertainties.

Results for a representative dive indicate the modified GSM had lower error throughout much of the dive compared to the standard GSM (Figure 2.11b). The modified GSM also removed the rapid spike in error occurring near apogee (minute 15-16) in the standard GSM. The modified GSM in which range data was used to correct the start and end locations of the dive (i.e. GPS and surface drift errors removed) is also shown in Fig. 2.11b for comparison. This solution, labeled 'mod GSM (w/GPS corr)', represents the theoretical expected error in the modified GSM solution if dive start and end locations were known exactly.

The modified GSM was applied to all the tracked dives from the Dabob Bay experiment using attitude data from the stock compass. The averaged error metrics for the modified GSM solution and the modified GSM with corrected GPS locations are compared to those for the standard GSM solution in Table 2.4. Results

Table 2.4
Modified GSM
Average Error Metrics (with 1σ standard deviation)

	Max Error (m)	RMS Error (m)	Norm. Max Error (%)
SG GSM	21.6 (5.6)	12.7 (3.5)	4.3 (1.9)
Mod GSM	16.5 (5.3)	9.8 (3.1)	3.2 (1.0)
Mod GSM (w/GPS corr)	13.0 (5.8)	7.2 (3.5)	2.4 (0.8)

indicate the modifications improved accuracy of the GSM localization solution for the Dabob Bay experiment.

2.7 Conclusion and Future Work

Both the Seaglider's GSM and HDM localization solutions were evaluated with regards to a ground truth tracked path from the Dabob Bay tracking range. The GSM solution was consistently closer to the tracked path, and thus the GSM was used to evaluate effects of inertial measurements on solution accuracy.

This paper quantifies the accuracy of a number of different localization solutions for the Seaglider AUV and identifies various sources of error present in these solutions. The evaluated solutions rely on attitude estimates using data from two different compasses: the Seaglider's stock Sparton compass and the experimentally integrated Lord AHRS/IMU. The Seaglider's GSM solution using the stock compass was determined to have the smallest deviations from the ground truth range track, with an average horizontal error of 12.7 m rms for a 90 m dive.

The incorporation of additional inertial measurements from the IMU did not provide significant improvements in the localization accuracies of the GSM solution. Some of the error present in solutions relying on data from the IMU was a result of sensor misalignment and magnetic disturbances from the magnetic field of the Seaglider's battery. Solutions and simulations removing effects of these error

sources show insignificant improvements (less than 10 cm reduction in rms error) would be expected from using IMU attitude estimates in place of the current stock compass.

Error in the HDM solution primarily results from errors in the model which cause inaccurate velocity estimates throughout much of the dive. Errors in the GSM solution were found to result from a combination of uncertainties in the GPS fixes at the surface, surface drift occurring between the GPS fixes and start/end of the dive, errors in attitude estimates, and other errors in the model assumptions, particularly near the apogee phase of the dive. Based on these identified sources of error, a modified GSM localization solution was developed which resulted in lower error metrics and standard deviation values than any currently available or inertial based localization solution.

Future analysis will incorporate ADCP measurements from the Seaglider to simultaneously estimate the velocity of the Seaglider and the water current profile for each dive. These velocity measurements could then be used in dead-reckoning localization solutions or to aid an inertial navigation solution. Since ADCP measurements on gliders are still relatively novel, additional experiments to validate the measured current profiles would also be an important step in development of these solutions.

A better understanding of vehicle dynamics during apogee would aid in developing glider localization models. The apogee phase of the dives showed large increases in localization error due to a breakdown of the model assumptions. Better characterization of vehicle dynamics during this phase of the dive could help develop a better vehicle model.

A similar data set collected in deeper water would provide an opportunity to validate these modifications and could help develop a better understanding of

how the various errors in the models scale with dive depth. Such a data set could be completed at a facility like the Atlantic Undersea Test and Evaluation Center (AUTEC) in the Bahamas or using a small ultra-short baseline (USBL) system with a transponder small enough to fit in the Seaglider's payload bay.

Acknowledgment

The authors would like to thank the Seaglider group at Kongsberg Underwater Technologies Inc for their assistance with the integration of the sensor and datalogger on the Seaglider, the Naval Undersea Warfare Center Division Keyport for their support of the acoustic range tracking experiment and the University of Rhode Island Ocean Engineering Department.

This project was completed as part of Wendy Snyder's Master's thesis under the support of the Science, Mathematics, and Research for Transformation (SMART) scholarship program and the Office of Naval Research award N00014-17-1-2228.

List of References

[1] C.C. Eriksen, T.J. Osse, R.D. Light, T. Wen, T.W. Lehman,P.L. Sabin, J.W. Ballard, A.M. Chiodi, "Seaglider: A long-range autonomous underwater vehicle for oceanographic research," *IEEE Journal of Oceanic Engineering*, 2001.

[2] L. J. Van Uffelen, E. M. Nosal, B. M. Howe, G. S. Carter, P. F. Worcester, M. A. Dzieciuch, K. D. Heaney, R. L. Campbell, P. S. Cross, "Estimating uncertainty in subsurface glider position using transmissions from fixed acoustic tomography sources," *Journal of the Acoustical Society of America*, 2013.

[3] L. J. Van Uffelen, B. M. Howe, E. M. Nosal, G. S. Carter, P. F. Worcester, M. A. Dzieciuch, "Localization and subsurface position error estimation of gliders using broadband acoustic signals at long range," *IEEE Journal of Oceanic Engineering*, 2016.

[4] L. Medagoda, S. B. Williams, O. Pizarro, J. C. Kinsey, and M. V. Jakuba, "Mid-water current aided localization for autonomous underwater vehicles," *Autonomous Robots*, 2016.

[5] Hegrens, and O. Hallingstad, "Model-aided ins with sea current estimation for robust underwater navigation," *IEEE Journal of Oceanic Engineering*, 2011.

[6] Stanway, Jordan M., "Dead reckoning through the water column with an acoustic doppler current profiler: Field experiences," *Oceans 2011*, 2011.

[7] W. Snyder, L. Van Uffelen, and M. Renken, "Effects of incorporating inertial measurements on the localization accuracy of the Seaglider AUV," *Oceans 2019*, 2019.

[8] P. D. Groves, *Principles of GNSS, Inertial, and Multisensor Intergrated Navigation Systems.* Artech House, 2008.

[9] W. Li and J. Wang, "Effective adaptive kalman filter for mems-imu magnetometers integrated attitude and heading reference system," *The Journal of Navigation*, vol. 66, pp. 99–113, 2013.

[10] J. Diebel, "Representing attitude: Euler angles, unit quaternions, and rotation vectors," *Matrix*, vol. 58, 2006.

APPENDIX

Fiber Optic Gyroscope Simulation

Both the Seaglider's Sparton compass and the Lord EKF have the greatest uncertainty in the heading estimate which is used to determine the direction the vehicle is moving in the north-east plane. As a result, errors in heading can lead to errors in the north-east position as evidenced by the simulation results (Figure 2.9). While depth position errors can be corrected using measurements from the pressure sensor, north-east errors rely on relatively infrequent GPS fixes for correction.

One alternative to MEMS gyroscopes are FOGs which typically have lower noise and drift rates resulting in more accurate and reliable measurements. The initial plan for this project included testing the effects of a single-axis FOG on heading estimates; unfortunately, no usable data was collected from the FOG installed on the Seaglider during the Dabob Bay experiment.

Instead, the simulation used to estimate effects of attitude errors on the overall error was repeated for a scenario in which a FOG was available for heading-aiding. Angular rate measurements about the z axis (body frame) were simulated using noise specifications for the KVH DSP-1760 single-axis fiber optic gyroscope. The resulting simulated measurements were fused with the simulated measurements from the Lord IMU to get a complete attitude estimate. The sensor fusing algorithm incorporated a tilt compensation to account for the gyroscope being rotated as the glider pitched and rolled as well as a Kalman filter to combine gyroscope measurements from the FOG with magnetic heading estimates from the Lord IMU.

The simulation compared an ideal GSM solution with no sensor noise to GSM solutions in which attitude inputs included sensor noise. Figure A.1a shows the simulated error for the Lord IMU (blue), FOG-aided Lord IMU (red) and the

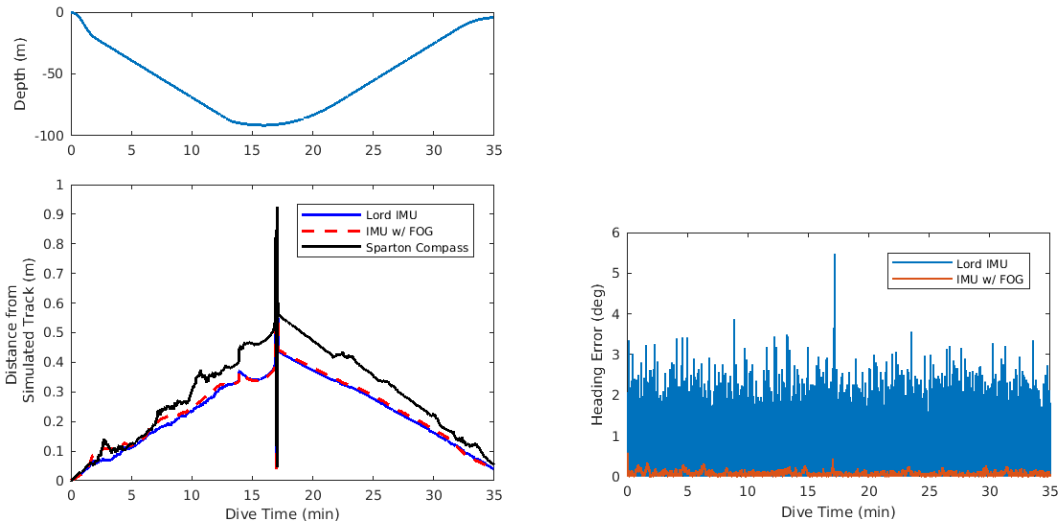

(a) Localization Error

(b) Heading Error

Figure A.1: (a) Simulated localization error for the GSM using attitude inputs from the Sparton compass (black) and the Lord IMU with (red) and without (blue) aiding from a single-axis fiber optic gyroscope on the heading axis. (b) Magnitude of simulated heading error with (red) and without (blue) aiding from the fiber optic gyroscope.

Seaglider Sparton compass (black). The magnitude of the heading error for the Lord IMU and FOG-aided Lord IMU heading estimates as a function of dive time is shown in Figure A.1b. While the incorporation of measurements from the single-axis FOG does significantly reduce noise in the heading estimate, it does not appear to have significant effect on the localization accuracy. Most likely, noise in the heading estimate without the FOG cancels itself out as it is incorporated into the dead-reckoned solution resulting in a similar localization estimate even when attitude noise is reduced from the FOG-aiding.